

Optimal Power Flow for Unbalanced Bipolar DC Distribution Grids

Mackay, Laurens; Guarnotta, Robin; Dimou, Anastasios; Morales-Espana, German; Ramirez-Elizondo, Laura; Bauer, Pavol

DOI

[10.1109/ACCESS.2018.2789522](https://doi.org/10.1109/ACCESS.2018.2789522)

Publication date

2018

Document Version

Accepted author manuscript

Published in

IEEE Access

Citation (APA)

Mackay, L., Guarnotta, R., Dimou, A., Morales-Espana, G., Ramirez-Elizondo, L., & Bauer, P. (2018). Optimal Power Flow for Unbalanced Bipolar DC Distribution Grids. *IEEE Access*, 6, 5199-5207. <https://doi.org/10.1109/ACCESS.2018.2789522>

Important note

To cite this publication, please use the final published version (if applicable). Please check the document version above.

Copyright

Other than for strictly personal use, it is not permitted to download, forward or distribute the text or part of it, without the consent of the author(s) and/or copyright holder(s), unless the work is under an open content license such as Creative Commons.

Takedown policy

Please contact us and provide details if you believe this document breaches copyrights. We will remove access to the work immediately and investigate your claim.

Optimal Power Flow for Unbalanced Bipolar DC Distribution Grids

Laurens Mackay, *Student Member, IEEE*, Robin Guarnotta, Anastasios Dimou, Germán Morales-España, *Member, IEEE*, Laura Ramirez-Elizondo, *Member, IEEE*, and Pavol Bauer, *Senior Member, IEEE*

Abstract—The emergence of distributed energy resources can lead to congestion in distribution grids. DC distribution grids are becoming more relevant as more sources and loads connected to the low voltage grid use dc. Bipolar dc distribution grids with asymmetric loading can experience partial congestion resulting in a nodal price difference between the two polarities if a respective market model is applied. In order to take into account this price difference, this paper presents an optimal power flow (OPF) model formulated in terms of voltage and current. In the case of bipolar dc distribution grids, the single line approximation is no longer valid because current can flow in the neutral conductors as well. Moreover, loads and sources can be connected between any two nodes in the network. The proposed exact OPF formulation includes bilinear equations. The locational marginal prices (LMP) are derived by linearizing the problem at the optimal solution. Example cases show the various phenomena that can appear under asymmetric loading, such as pole-to-pole connections combined with pole-to-neutral connections, parallel sources, meshed grids and their effect on the LMP.

Index Terms—DC distribution grid, optimal power flow, congestion management, locational marginal prices

NOMENCLATURE

Indices and Sets

$\mathcal{N} = \mathcal{N}_+ \cup \mathcal{N}_- \cup \mathcal{N}_N$	Positive, negative and neutral nodes.
\mathcal{N}^\emptyset	Nodes \mathcal{N} without reference node.
$m, n \in \mathcal{N}$	Nodes of the bipolar grid.
$(m, n) \in \mathcal{G}$	Pair of nodes with connecting line.
$(m, n, s) \in \mathcal{S}$	Individual sources s at nodes (m, n) .

Variables

u_m	Voltage at node m [V].
i_m	Total current at node m , going from the source layer into the resistive network [A] (see Fig. 3).
$i_{m,n}$	Line current from node m to n [A].
$i_{m,n,s}^S$	Current of one source, defined as negative (−), or a load defined as positive (+) [A].
$p_{m,n,s}^S$	Power of source s connected at (m, n) [W].
λ_m^I	LMP for node m in terms of current [m.u./Ah].
$\lambda_{m,n}^P$	LMP for nodes (m, n) in terms of power [m.u./Wh].
$(\cdot)^*$	Superscript for variable value at optimal solution.

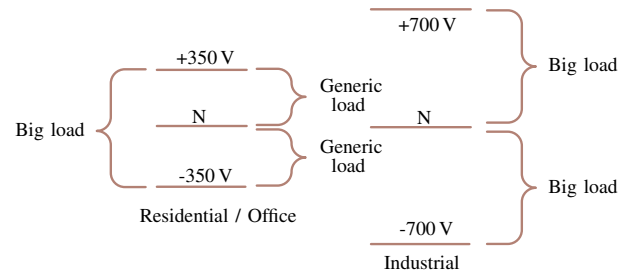


Fig. 1. Modular bipolar LVdc voltage levels and how devices could be connected [2].

Parameters

$G_{m,n}$	Branch conductance [S].
\underline{U}, \bar{U}	Voltage limits for both poles [V].
$\underline{U}_N, \bar{U}_N$	Voltage limits for neutral conductor [V].
$\underline{I}_{m,n}, \bar{I}_{m,n}$	Line current limits [A].
$\underline{I}_{m,n,s}^S, \bar{I}_{m,n,s}^S$	Current limits for source [A].
$\underline{P}_{m,n,s}^S, \bar{P}_{m,n,s}^S$	Power limits for source [W].
$\Pi_{m,n,s}^S$	Marginal cost/value of sources [m.u./Wh].

I. INTRODUCTION

DISTRIBUTION GRIDS are expected to experience more congestion problems due to the emergence of electrical vehicles, renewable energy sources, and other distributed energy resources. Locational marginal prices (LMP) can enable optimal utilization of distributed energy resources owned by different entities. DC distribution grids have advantages over ac distribution grids due to their inherently higher power transfer capacity, and due to the fact that most loads and sources connected to the low voltage grid nowadays are already dc. In the future, more and more, will be either inherently dc or use a dc link to couple variable rotation speeds [1].

Bipolar dc grids have a neutral conductor in addition to the positive and negative conductor of unipolar dc grids. Their configuration can be compared to that of a 3-phase or 2-phase ac grid. As shown on the left side of Fig. 1, small devices can be connected between the positive pole and the neutral or between the neutral and the negative pole. Without loss of generality, in this paper a nominal voltage of ± 350 V is

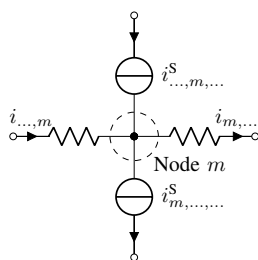


Fig. 2. Traditional representation of a node with connected lines and sources that can be either generators or loads. This is split up into layers as shown in Fig. 3.

assumed [1]. Bigger devices can be connected directly between the positive pole and the negative pole. Therefore, a voltage of 700 V is available to these devices. The power available on a 700 V dc connection corresponds to the one of a 400 V 3-phase ac connection with same rms current rating I , while using one wire less ($\sqrt{3} \cdot 400 \text{ V} \cdot I = 693 \text{ V} \cdot I \approx 700 \text{ V} \cdot I$). For bigger industrial applications, e.g., photovoltaic power plants, a bipolar 700 V grid can be made as shown on the right side of Fig. 1 [2].

Bipolar dc distribution grids offer twice the power transfer capacity (+100%) of unipolar dc grids, while only one conductor is added (+50%). The total losses in a balanced system remain the same as does the voltage rating of the small devices. Small devices in general have galvanic isolation inside or do not refer their potential to ground. Therefore, no increase in component cost is expected. If a balancing converter between both polarities is added, longer distances can be bridged without requiring a neutral conductor, thus saving additional 33% of conductor material.

Optimal power flow (OPF) is a method to optimize the dispatch of generation and load in order to minimize the total cost or maximize the social welfare while respecting operation limits. In literature for bipolar dc grids, OPF has been done for HVdc and a combined approximated OPF for hybrid ac and dc networks [3], [4], [5]. Bipolar HVdc lines are normally operated symmetrically, hence a single line approximation can be used in these dc networks [6]. DC microgrid literature contains a vast amount of research on local energy management systems. Mostly local dc nano- or microgrids are considered where network constraints are not included [7] and, if they are, only unipolar dc grids are considered [8].

In bipolar dc distribution grids [1] the lines can be loaded asymmetrically (unbalanced), i.e., devices connected between pole and neutral, to allow smaller devices to connect to lower voltage. Due to this likely asymmetric loading of both polarities in distribution grids, partial line congestion can appear. Congestion of distribution grids occur when power flows are subject to physical or operational limitations. These are likely to occur in distribution networks in the future due to the increase of installed power capacity (e.g. electric vehicles and photovoltaics). Partial line congestion means that for example only the positive pole is overloaded while more power could be transferred on the negative pole. Moreover, asymmetric congestion should result in differing LMP on the two polarities at the same location. Furthermore, parts of the

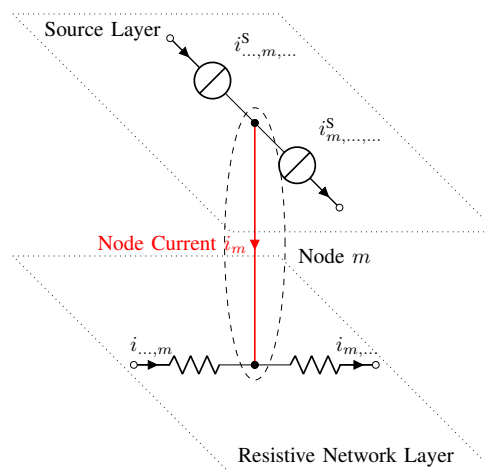


Fig. 3. The node from Fig. 2 with connected lines and sources split up into source layer (top) and resistive network layer (bottom). The node current i_m connects both layers in every node. It represents the total current flowing into the resistive network from all generators and loads connected in the source layer. This current i_m is used for deriving the LMP.

grid may be built with only one of the two polarities, or the neutral conductor can be left out for longer distances. The voltages in the low voltage grid can have significant variations due to losses and have to be kept within bounds.

This paper proposes a method to model the OPF problem for unbalanced bipolar dc grids. It can also be used for bipolar dc grids under symmetric loading. The problem is formulated in terms of voltage and current, instead of the usual formulation in power. The formulation does not use the usual single line approximation, as the current in the neutral conductor influences the potentials of the neutral nodes. The present paper builds up on previous work [9], however, the LMP results are different. Instead of only fixing the voltage at the optimal solution, this paper uses a first order linearization. This ensures the same optimal solution in the linear program. Thereby the applicability is extended and allows for the optimization of meshed grids, which was not possible before. The new formulation leads to the incorporation of marginal losses into the LMP, which means that the current prices within non-congested areas are no longer equal. Furthermore the proposed mathematical formulation is more precise and allows multiple sources at the same location. More complex examples and special cases can therefore be demonstrated.

The remainder of this paper is organized as follows. Section II introduces the modeling method without single line model. Based thereon, the exact OPF problem is formulated and the LMP are derived in Section III. In Section IV some numerical example cases are presented in order to demonstrate the methodology developed. Finally, in Section V conclusions are drawn and future work is identified.

II. MATHEMATICAL MODEL OF THE EXACT POWER FLOW IN BIPOLAR DC DISTRIBUTION GRIDS

Instead of the usual OPF representation in terms of power [6], in this paper the problem is formulated in terms of currents and voltages. In this way, constraints can be formulated as upper and lower bounds in terms of currents and voltages.

The network of sources and lines, as shown in Fig. 2, is split into a resistive network and a source layer, as illustrated in Fig. 3. This is done by putting all lines into the resistive layer and all loads and generators into the source layer. The resistive grid is modeled similar to the traditional dc OPF. The source layer structures the positive and negative connections of all sources and loads and assigns them to the right nodal current. This nodal current i_m links both layers and is used later for the derivation of the LMP.

A. Modeling of the Grid

The exact linear power flow in the network is represented by explicitly modeling voltage and current variables. The voltage magnitude differences between two nodes and the respective resistances of the connecting branches impose the current flow pattern [4].

The bipolar dc grid consists of the nodes in set \mathcal{N} , for which the following equations are true:

$$i_{m,n} = G_{m,n} \cdot (u_m - u_n) \quad \forall (m,n) \in \mathcal{G} \quad (1)$$

$$i_m = \sum_{n|(m,n) \in \mathcal{G}} i_{m,n} - \sum_{n|(n,m) \in \mathcal{G}} i_{n,m} \quad \forall m \in \mathcal{N} \quad (2)$$

where node current i_m is equal to the algebraic sum of the currents flowing into the connected branches. This is the Kirchhof's current law of the resistive network at the bottom of Fig. 3.

B. Modeling Generators and Loads

In order to allow a more generic modeling of prosumers, that can both consume and produce power, loads are also modeled as sources. For a more elegant mathematical formulation later on, sources that feed power into the grid (generators) have negative current and power, while sources that consume power (loads) have positive current and power. All sources are modeled as current sources because they can be connected in parallel which would not be possible with voltage sources. The positive current of a current source (load) is defined as flowing from the more positive pole to the more negative pole. That means that current is extracted out of the resistive network at the positive pole and fed into the resistive network at the negative pole (Fig. 3).

In a bipolar grid, sources and loads can be connected between various points in the network: between positive polarity and neutral conductor, between neutral conductor and negative polarity conductor, or directly between positive and negative conductors, advisable for bigger sources and loads. It is evident that in actual applications this could lead to asymmetric loading of the grid, causing increased voltage magnitudes for the nodes of the neutral conductor. Therefore, also the neutral conductor is modeled and all sources and loads are connected between two nodes (m,n) .

Multiple sources connected to the same nodes could be useful, e.g., to model a building with PV together with the loads of the building. In order to allow multiple sources with different characteristics at the same location an additional sum is made over all individual sources between the same nodes.

The node currents are then the algebraic sum of all sources connected on a specific node m :

$$-i_m = \sum_{n|(m,n,s) \in \mathcal{S}} \sum_{s|(m,n,s) \in \mathcal{S}} i_{m,n,s}^S - \sum_{n|(m,n,s) \in \mathcal{S}} \sum_{s|(n,m,s) \in \mathcal{S}} i_{n,m,s}^S \quad \forall m \in \mathcal{N}^0 \quad (3)$$

Equations (2) together with (3) are essentially constituting Kirchhoff current law. The node current i_m is the variable used to describe the interface between the resistive network and the sources together with the loads connected on various nodes as shown in Fig. 3. For a node m of the system, where no current injection or extraction occurs due to the lack of a source or a load, the node current i_m will be zero. Otherwise the node current i_m , according to (3), is equal to the total balance of current injected and extracted from this specific node.

While the power flow in the network can be described fully by previous equations, the power of the sources will be necessary for modeling power limits and marginal cost in terms of energy. The power of the sources is

$$p_{m,n,s}^S = (u_m - u_n) \cdot i_{m,n,s}^S \quad \forall (m,n,s) \in \mathcal{S} \quad (4)$$

which is a bilinear equation, thus making the problem quadratic.

C. Limits

The reference node is assumed to be grounded and its voltage is fixed to zero:

$$u_0 = 0 \text{ V} \quad (5)$$

Under normal operating conditions the acceptable voltage variation is limited to certain percentage of the nominal operating voltage. Moreover, operational constraints due to line current limits are taken into account. The nodes of the network \mathcal{N} are divided into three groups: \mathcal{N}_+ for the positive pole, \mathcal{N}_- for the negative pole, and \mathcal{N}_N for the neutral conductor. The voltage and line current limits are

$$\underline{U} \leq u_m \leq \bar{U} \quad \forall m \in \mathcal{N}_+ \quad (6)$$

$$\underline{U} \leq -u_m \leq \bar{U} \quad \forall m \in \mathcal{N}_- \quad (7)$$

$$\underline{U}_N \leq u_m \leq \bar{U}_N \quad \forall m \in \mathcal{N}_N \quad (8)$$

$$\underline{I}_{m,n} \leq i_{m,n} \leq \bar{I}_{m,n} \quad \forall (m,n) \in \mathcal{G} \quad (9)$$

The sources can be constrained by current and power limits:

$$\underline{I}_{m,n,s}^S \leq i_{m,n,s}^S \leq \bar{I}_{m,n,s}^S \quad \forall (m,n,s) \in \mathcal{S} \quad (10)$$

$$\underline{P}_{m,n,s}^S \leq p_{m,n,s}^S \leq \bar{P}_{m,n,s}^S \quad \forall (m,n,s) \in \mathcal{S} \quad (11)$$

Current can be used to model the limits of power electronics while power is more appropriate for process limits. The separation of these two limits may be preferable when significant voltage deviations appear in the distribution grids. The power constraint (11) is an indirectly a quadratic inequality constraint due to (4) being quadratic.

III. OPTIMAL POWER FLOW

After modeling the grid, sources and constraints, the OPF is solved in order to minimize total cost. A two-step method following a similar approach as that in [10] is used to solve the economic dispatch and derive the LMP. Firstly the exact model is used to find the optimal solution. Secondly the problem is linearized at the found optimal solution to derive the LMP.

A. Cost/Value Function of Sources

The operation cost of each generator and load is defined by a given marginal cost $\Pi_{m,n,s}^S$ (cost of increasing the output by one unit). Demand response of loads could be implemented by giving them a marginal value (defined as opposite of marginal cost) and allowing its power consumption to be variable. Load shedding with different priorities could also be implemented by giving different values to loads. If the resulting price is higher, they would automatically turn off [1].

B. Solving for the Economic Dispatch

The optimal economic dispatch is found by minimizing the total cost and this is equivalent to maximizing the social welfare [11]. The problem formulation is presented as follows:

$$\begin{aligned} \min \quad & \sum_{(m,n,s) \in \mathcal{S}} -p_{m,n,s}^S \cdot \Pi_{m,n,s}^S \\ \text{s.t.} \quad & (1) - (11) \end{aligned} \quad (12)$$

The choice of sign is important for the marginal values used in the next section. The multiplication of the two variables in (4) makes the problem bilinear, a special case of quadratic programming for which the problem is not convex.

It is important to note that due to the non-convexity of the problem, an optimal solution is not guaranteed to be the global optimum. This aspect has to be dealt with by the optimization algorithm, which is not in the scope of this paper. It is assumed that the found solution is acceptable because it is feasible, even though it is possibly not globally optimal.

C. Locational Marginal Prices (LMP)

Non-convex problems suffer from a weak duality between. In order to derive the LMP for the non-convex problem, the problem is linearized at the optimal solution [10].

1) *Linearization*: Firstly, the quadratic problem (12) is solved and the optimal voltages u_m^* and source currents $i_{m,n,s}^{S*}$ are obtained. Then, the problem is linearized around this optimal solution. This means that power equation (4), the only non-linear equation in the problem, has to be linearized. By using the first order Taylor approximation this finally results in

$$\begin{aligned} p_{m,n,s}^S &= (u_m^* - u_n^*) \cdot i_{m,n,s}^{S*} \\ &+ (u_m - u_n) \cdot i_{m,n,s}^{S*} \\ &- (u_m^* - u_n^*) \cdot i_{m,n,s}^{S*} \end{aligned} \quad \forall (m, n, s) \in \mathcal{S} \quad (13)$$

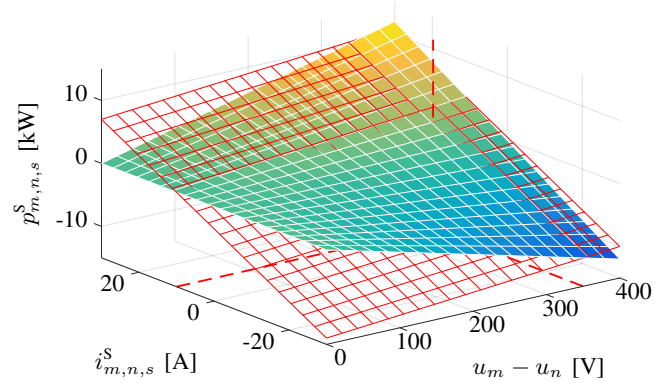


Fig. 4. Visualization of the linearization around the solution of the bilinear power equation (surface). The linearized power equation (at 350 V, 10 A) is shown as red mesh.

In Fig. 4 a visualization of the bilinear power equation (4) and its linearization (13) is shown. Herewith a linear optimization problem can be formulated as

$$\begin{aligned} \min \quad & \sum_{(m,n,s) \in \mathcal{S}} -p_{m,n,s}^S \cdot \Pi_{m,n,s}^S \\ \text{s.t.} \quad & (1) - (3), (13), (5) - (11) \end{aligned} \quad (14)$$

The problem formulation (14) is now linear, thus convex and with strong duality. The linear problem is initialized at the solution of (12). In this way, the same solution is obtained, also for the case of multiple solutions at the same optimum. In other words, the variables computed using linear programming are then the same as for quadratic programming. The linearization is thus exact at the solution. Therefore, the dual variables can be used to derive the LMP for the original problem [12].

LMP is the marginal cost of supplying the next increment of energy at a given location. LMP are commonly expressed in terms of power and reflect also losses and congestion [13], [14], [15]. In this case, dual variables obtained from the equality constraint (2) for each node are given in terms of current (instead of power) and denoted by λ_m^I . Using linear programming enables to interpret these dual variables as the LMP for all m . However they are in terms of current [m.u./Ah], which is not the usual unit (m.u. stands for Monetary Unit).

2) *LMP in Terms of Power*: LMP in power terms are calculated for all generators and loads connected between different polarities $m, n \in \mathcal{N}$. Their value can be derived as follows: Let $\alpha_{m,n,s}$ be the amount payable by a prosumer per time interval, which is by definition the power times the LMP:

$$\alpha_{m,n,s} = p_{m,n,s}^S \cdot \lambda_{m,n}^P \quad (15)$$

On the other hand this amount has to be equal to the amount payable for extracting the source current $i_{m,n,s}^{S*}$ in one node and injecting it in the other, because that is what is physically happening:

$$\begin{aligned} \alpha_{m,n,s} &= \lambda_m^I \cdot i_{m,n,s}^{S*} + \lambda_n^I \cdot (-i_{m,n,s}^{S*}) \\ &= (\lambda_m^I - \lambda_n^I) \cdot i_{m,n,s}^{S*} \end{aligned} \quad (16)$$

TABLE I
LINE CURRENTS

	\mathcal{N}_+		\mathcal{N}_N		\mathcal{N}_-	
Case 1	$i_{4,5}$	68.03	$i_{0,1}$	29.66	$i_{8,9}$	-97.69
	$i_{5,6}$	40.67	$i_{1,2}$	29.33	$i_{9,10}$	-70.00
	$i_{6,7}$	-0.48	$i_{2,3}$	-0.70	$i_{10,11}$	1.18
Case 2	$i_{2,3}$	13.62	$i_{0,1}$	-13.62	$i_{5,6}$	0.00
	$i_{3,4}$	-22.51	-	-	$i_{6,7}$	22.51
Case 3	$i_{3,4}$	70.00	$i_{0,1}$	0.00	$i_{6,7}$	-70.00
	$i_{4,5}$	-40.96	$i_{1,2}$	5.96	$i_{7,8}$	35.00
	$i_{3,5}$	29.04	$i_{0,2}$	5.96	$i_{6,8}$	-35.00

TABLE II
NODE VOLTAGES

	\mathcal{N}_+		\mathcal{N}_N		\mathcal{N}_-	
Case 1	u_4	367.50	u_0	0.00	u_8	-367.50
	u_5	364.10	u_1	-1.48	u_9	-362.62
	u_6	360.03	u_2	-4.42	u_{10}	-355.62
	u_7	360.06	u_3	-4.38	u_{11}	-355.67
Case 2	u_2	367.06	u_0	0.00	u_5	-332.50
	u_3	366.37	u_1	0.68	u_6	-332.50
	u_4	367.50	-	-	u_7	-333.63
Case 3	u_3	367.50	u_0	0.00	u_6	-367.50
	u_4	360.50	u_1	0.00	u_7	-360.50
	u_5	364.60	u_2	-0.60	u_8	-364.00

By solving (15) for $\lambda_{m,n}^P$ and substituting (16) and (4), the LMP in terms of power between nodes (m, n) can be derived as

$$\lambda_{m,n}^P = \frac{\alpha_{m,n,s}}{P_{m,n,s}^S} = \frac{(\lambda_m^I - \lambda_n^I) \cdot i_{m,n,s}^S}{(u_m - u_n) \cdot i_{m,n,s}^S} \quad \forall m, n \in \mathcal{N} \quad (17)$$

$$= \frac{\lambda_m^I - \lambda_n^I}{u_m - u_n}$$

So the LMP between two nodes in terms of power is equal to the difference of current LMP λ_m^I divided by the voltage difference of the nodes u_m .

3) *Marginal Losses*: Using the marginal values of the OPF as LMP, includes marginal losses into the price. Thereby the losses have a greater impact on the price than the physical power loss. The marginal losses are approximately twice as high as the cost of the physical losses. This phenomenon is known from literature for ac grids [16] and is therefore not further discussed in this paper.

IV. NUMERICAL EXAMPLES

This section presents three cases that were selected to show the special phenomenon that can occur in bipolar dc grids with asymmetric loading, which cannot be modeled using OPF with single line approximation. Case 1 illustrates the method and shows partial congestion on only one line of a bipolar cable. Case 2 shows the effect of sources connected directly between two poles, and multiple sources between the same nodes, as well as interdependence between the two poles. Case 3 shows a meshed grid with partial line congestion. In this last case the LMP on the non-congested lines are of special interest.

The problems are modeled using GAMS and solved using the CONOPT solver [17]. The networks consist of 25 mm² cables with $\bar{I}_{m,n} = -\underline{I}_{m,n} = 70$ A current limit and 50 mm² cables with $\bar{I}_{m,n} = -\underline{I}_{m,n} = 100$ A current limit. The voltage limits are set to 350 V \pm 5% and the neutral conductor has the same operating range:

$$\bar{U} = 367.5 \text{ V}$$

$$\underline{U} = 332.5 \text{ V}$$

$$\bar{U}_N = 17.5 \text{ V}$$

$$\underline{U}_N = -17.5 \text{ V}$$

The upper nodes of Fig. 5, 6 and 7 are in \mathcal{N}_+ , the lower nodes in \mathcal{N}_- , and the nodes in the middle are in \mathcal{N}_N .

Each case has its own tables to show specific configuration of loads and generators, and LMP. Table I presents the line currents for all cases. Table II shows the nodal voltages.

A. Case 1: Bipolar Grid with Partial Line Congestion

The goal of this case is to show the congestion of only one of three conductors in a line. Fig. 5 shows the example grid. The central 4 sources operate as loads. On the left and the right each two generators are connected between neutral and the poles. Table III shows the marginal costs $\Pi_{m,n,s}^S$ of the generators. The left ones are cheap (5 m.u./kWh) while the right ones are expensive (10 m.u./kWh). The power limits of the generators on the right are -20 kW and on the left -25 kW on top and -50 kW on the bottom. The loads in the middle on the left side are fixed to 10 kW and on the right side on the top 15 kW and on the bottom 25 kW. The lines on the left and right are 100 m long and have 50 mm² cross section with a current limit $\bar{I}_{m,n}$ of 100 A. The lines in the middle between the two loads have the same length but are thinner and have a current limit of 70 A which is reached on the negative conductor $i_{9,10}$ as can be seen in Table I.

Table IV displays the voltage differences $u_m - u_n$ and the LMP of each connection point. The LMP are shown in terms of power ($\lambda_{m,n}^P$) and also in terms of current for both connecting nodes (λ_m^I and λ_n^I).

On top, for the positive conductor, the locational marginal price is related to the expensive generator at the right, which is needed only to cover the losses. The line current $i_{6,7}$ is so low that almost no losses occur and due to rounding the price at (6,2) is the same. The current in the neutral conductor $i_{2,3}$ even slightly overcompensates for these losses in the positive conductor such that the price is slightly lower (9.999 rounded to 10.00). Further to the left, the power is flowing from the left hand side and hence prices decrease due to less losses on the way.

On the negative conductor at the bottom, a line congestion occurs and $i_{9,10}$ is limited to -70 A. This is not the case for the neutral conductor, as positive and negative currents are

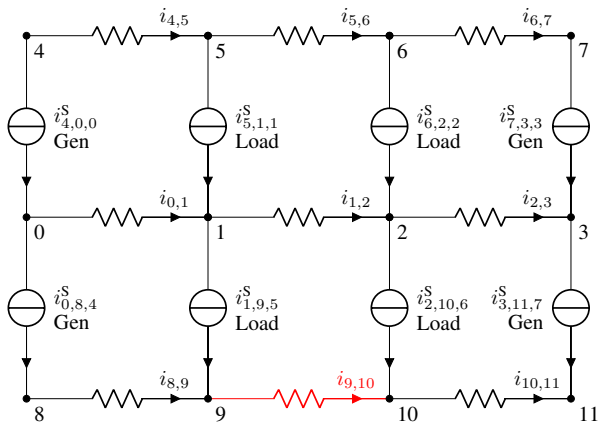


Fig. 5. Bipolar dc grid with positive (top), neutral (middle) and negative conductors (bottom). The 4 central sources are loads while the 4 outer sources are generators. A line congestion occurs on $i_{9,10}$ in the middle.

TABLE III
CASE 1: SOURCE VARIABLES

Parameter / Variables	Sources' Inputs and Outputs			
	$(\mathcal{N}_+, \mathcal{N}_N)$	$(5,1,1)$	$(6,2,2)$	$(7,3,3)$
$\Pi_{m,n,s}^S$ [m.u./kWh]	5	0	0	10
$\underline{P}_{m,n,s}^S$ [kW]	-25	10	15	-20
$\overline{P}_{m,n,s}^S$ [kW]	0	10	15	0
$p_{m,n,s}^S$ [kW]	-25.00	10.00	15.00	-0.18
$i_{m,n,s}^S$ [A]	-68.03	27.35	41.16	-0.48
Parameter / Variables	Sources' Inputs and Outputs			
	$(\mathcal{N}_N, \mathcal{N}_-)$	$(1,9,5)$	$(2,10,6)$	$(3,11,7)$
$\Pi_{m,n,s}^S$ [m.u./kWh]	5	0	0	10
$\underline{P}_{m,n,s}^S$ [kW]	-50	10	25	-20
$\overline{P}_{m,n,s}^S$ [kW]	0	10	25	0
$p_{m,n,s}^S$ [kW]	-35.90	10.00	25.00	-0.42
$i_{m,n,s}^S$ [A]	-97.60	27.69	71.18	-1.18

TABLE IV
CASE 1: LOCATIONAL MARGINAL PRICES

$(m, n) \in \mathcal{N}$	(4, 0)	(5, 1)	(6, 2)	(7, 3)
$u_m - u_n$ [V]	367.50	365.58	364.45	364.44
$\lambda_{m,n}^P$ [m.u./kWh]	9.82	9.94	10.00	10.00
λ_m^I [m.u./Ah]	3607.36	3641.28	3681.95	3681.71
λ_n^I [m.u./Ah]	0.00	8.33	37.70	37.35
$(m, n) \in \mathcal{N}$	(0, 8)	(1, 9)	(2, 10)	(3, 11)
$u_m - u_n$ [V]	367.50	361.13	351.20	351.29
$\lambda_{m,n}^P$ [m.u./kWh]	5.00	5.23	10.01	10.00
λ_m^I [m.u./Ah]	0.00	8.33	37.70	37.35
λ_n^I [m.u./Ah]	-1837.50	-1879.76	-3476.18	-3475.59

superimposed. The prices on the both sides on the congestion diverge. The left side is fed by generator (0,8,4) and the LMP increases due to the losses at (1,9). Additional supply is needed from the right generator and, with some additional losses, the LMP at (2,10) is slightly above the marginal cost of the generator.

This case presented the partial congestion (in line $i_{9,10}$) which only appears in unbalanced bipolar dc grids. This congestion cannot be modeled and observed with traditional OPF formulations.

B. Case 2: Parallel Sources, Pole to Pole Source and Demand Response

Fig. 6 shows the example grid for Case 2. All lines are 100 m long and 50 mm² thick. The two sources on the left are generators with a marginal cost as shown in Table V. In the middle there are two loads in parallel on the positive conductor. They implement demand response with variable power between 0 and $\overline{P}_{m,n,s}^S$ by setting a constant marginal value to $\Pi_{m,n,s}^S$ which is below the generator cost for the left load and above the for the right one. The bottom load also can apply demand response with a maximum power of only 7.5 kW. On the right a renewable energy source with zero marginal cost and plenty of supply capacity is connected directly from positive pole to negative pole.

The voltage differences $u_m - u_n$ and the LMP of each connection point are shown in Table VI. This case is constructed in order to show the challenges in asymmetric bipolar grids. While energy could be provided at zero cost in the system, still not all load can be supplied at the given willingness to pay. The load on the bottom and a part of the right top load is supplied by the zero marginal cost generator between two poles. The load on the bottom is at maximum power, therefore there is no path for additional current to the negative pole. The voltages difference on the negative pole is reduced to the limit in order to increase the current for the same power to the maximum.

On the positive pole the generator on the left supplies maximum power at a relatively high price to meet the demands of the right load (3,1,2). The LMP are defined by the willingness to pay of the right load. The price at the left generator is a bit lower due to the losses in between. The LMP on the negative pole are negative because an increase in load there would allow a higher current through load (3,1,2) and thus to generate more value. This means that loads/consumers receive money for their consumption. The prices are even more negative than the marginal value because, for an increase in load on the positive pole, less power is needed on the negative pole due to the lower voltage difference there. The price between positive and negative conductor is zero due to the available renewable energy from source (4,7,5).

C. Case 3: Meshed Bipolar Grid with Congestion

Fig. 7 shows the meshed bipolar dc grid for Case 3. The two sources on the left are generators with a marginal cost of zero as shown in Table VII. In the middle there are two loads with demand response. The top one has a high marginal

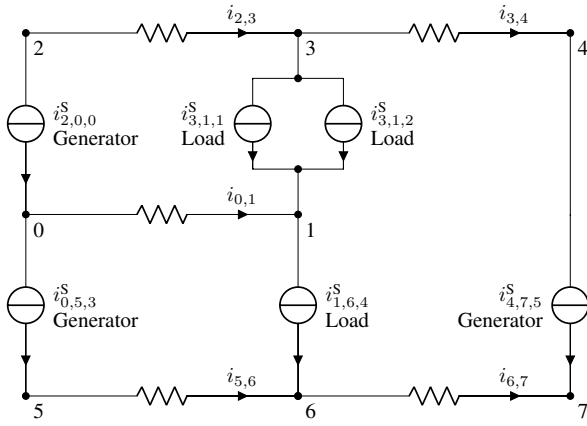


Fig. 6. Bipolar grid with parallel sources and a source from pole to pole. The two sources on the left and the one on the right are generators, the 3 sources in the middle are loads with varying value (demand response).

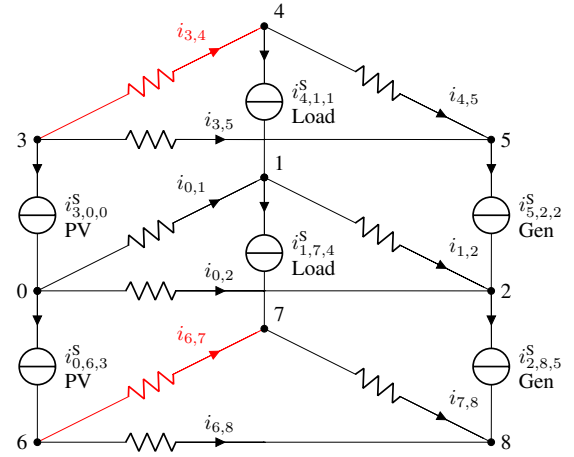


Fig. 7. Meshed bipolar dc grid with renewable sources on the left, variable loads in the middle and generators on the right.

TABLE V
CASE 2: SOURCE VARIABLES

Parameter / Variables	Sources' Inputs and Outputs			
	$(\mathcal{N}_+, \mathcal{N}_N)$	$(2,0,0)$	$(3,1,1)$	$(3,1,2)$
$\Pi_{m,n,s}^S$ [m.u./kWh]		5	3	10
$P_{m,n,s}^S$ [kW]		-5	0	0
$\bar{P}_{m,n,s}^S$ [kW]		0	10	15
$p_{m,n,s}^S$ [kW]		-5.00	0.00	13.21
$i_{m,n,s}^S$ [A]		-13.62	0.00	36.132
$(\mathcal{N}_N, \mathcal{N}_-) \text{ \& } (\mathcal{N}_+, \mathcal{N}_-)$				
	$(0,5,3)$	$(1,6,4)$	$(4,7,5)$	
$\Pi_{m,n,s}^S$ [m.u./kWh]		5	3	0
$P_{m,n,s}^S$ [kW]		-5	0	-20
$\bar{P}_{m,n,s}^S$ [kW]		0	7.5	0
$p_{m,n,s}^S$ [kW]		0.00	7.50	-15.78
$i_{m,n,s}^S$ [A]		0.00	22.51	-22.51

TABLE VI
CASE 2: LOCATIONAL MARGINAL PRICES

$(m, n) \in \mathcal{N}$	$(2, 0)$	$(3, 1)$	-
$u_m - u_n$ [V]	367.06	365.69	-
$\lambda_{m,n}^P$ [m.u./kWh]	9.86	10.00	-
λ_m^I [m.u./Ah]	3619.84	3626.55	-
λ_n^I [m.u./Ah]	0.00	-30.38	-
$(m, n) \in \mathcal{N}$			
	$(0, 5)$	$(1, 6)$	$(4, 7)$
$u_m - u_n$ [V]	332.50	332.50	710.13
$\lambda_{m,n}^P$ [m.u./kWh]	-10.84	-10.94	0.00
λ_m^I [m.u./Ah]	0.00	-30.38	3615.20
λ_n^I [m.u./Ah]	3602.88	3615.203	3615.203

TABLE VII
CASE 3: SOURCE VARIABLES

Parameter / Variables	Sources' Inputs and Outputs			
	$(\mathcal{N}_+, \mathcal{N}_N)$	$(3,0,0)$	$(4,1,1)$	$(5,2,2)$
$\Pi_{m,n,s}^S$ [m.u./kWh]		0	15	5
$P_{m,n,s}^S$ [kW]		-50	0	-50
$\bar{P}_{m,n,s}^S$ [kW]		0	40	0
$p_{m,n,s}^S$ [kW]		-36.40	40.00	-4.35
$i_{m,n,s}^S$ [A]		-99.04	110.96	-11.91
$(\mathcal{N}_N, \mathcal{N}_-) \text{ \& } (\mathcal{N}_+, \mathcal{N}_-)$				
	$(0,6,3)$	$(1,7,4)$	$(2,8,5)$	
$\Pi_{m,n,s}^S$ [m.u./kWh]		0	6	10
$P_{m,n,s}^S$ [kW]		-50	0	-50
$\bar{P}_{m,n,s}^S$ [kW]		0	40	0
$p_{m,n,s}^S$ [kW]		-38.59	37.85	0.00
$i_{m,n,s}^S$ [A]		-105.00	105.00	0.00

TABLE VIII
CASE 3: LOCATIONAL MARGINAL PRICES

$(m, n) \in \mathcal{N}$	$(3, 0)$	$(4, 1)$	$(5, 2)$
$u_m - u_n$ [V]	367.50	360.50	365.19
$\lambda_{m,n}^P$ [m.u./kWh]	0.00	10.16	5.00
λ_m^I [m.u./Ah]	0.00	3632.63	1813.34
λ_n^I [m.u./Ah]	0.00	-31.19	-12.62
$(m, n) \in \mathcal{N}$			
	$(0, 6)$	$(1, 7)$	$(2, 8)$
$u_m - u_n$ [V]	367.50	360.60	363.40
$\lambda_{m,n}^P$ [m.u./kWh]	0.00	6.00	2.98
λ_m^I [m.u./Ah]	0.00	-31.19	-12.62
λ_n^I [m.u./Ah]	0.00	-2194.19	-1097.10

value, while the bottom one has a low marginal value. On the right there are two more generators with, on top, relatively low marginal cost and, on bottom, high marginal cost. The lines are 100 m long, 25 mm² thick and have a current limit of ± 70 A. This current limit is reached for $i_{3,4}$ and $i_{6,7}$. Even though the other path is not congested, the power flow cannot be increased as the current distribution is defined by the difference in resistance. Current limiting devices [18] or power flow control converters [19] would allow an impedance adaption and better utilization of grid infrastructure. In this case however, the congestion leads to a price divergence as shown in Table VIII. The top right generator is producing additional power while the bottom one is too expensive for the bottom load, which does demand response instead.

The LMP on the negative pole are derived from the value of the curtailed load (1,7,4) as shown in Table VIII. At nodes (2,8) the LMP is a bit less than half of that value. If an additional unit of load would be connected here, the load (1,7,4) would only need to be reduced by half a unit as additional power can come directly from the source. This decrease will reduce the voltage drop in line (7,8), therefore the voltage drop in line (6,8) could be increased to supply the rest of the unit.

On the positive pole, the LMP are derived from the generator at the right. The LMP at the load is approximately double, because an increase in load by one unit would need an increase of generation at (5,2,2), which results in higher voltage drops in line (4,5). To keep the $i_{3,4}$ below its limit, the voltage difference from node 3 to 4 needs to stay the same. Hence, $i_{3,5}$ would have to be reduced and the loss in power needs to be additionally generated at (5,2,2). Therefore, approximately 2 units of power have to be provided at price 5.00 m.u./kWh for one additional unit of load. Due to marginal losses the price at the load is slightly more than double.

V. CONCLUSION

In this paper a method to exactly model bipolar dc distribution grids with asymmetric loading has been presented. This method can also be used for bipolar dc distribution grids with symmetric loading. The problem is formulated in terms of current and voltage instead of power in order to model the grid exactly and allows limits in voltages and currents. The objective function for the OPF problem is therefore bilinear. By linearizing the problem at the optimal solution, the LMP can be calculated. Different case studies showed how the LMP differ between the different polarities depending on the asymmetric loading and congestion. Moreover, connection to only positive and negative poles can lead to negative prices on one pole. The presented formulation can be used as a foundation for future application of LMP in bipolar dc distribution grids.

Future work includes the modeling of multiple voltage levels and the converters connecting them. Decentralized current limiters [18] or power flow control converters [19] could be included into meshed grids in order to better utilize the grid. Further, the operation of storage in the presented OPF formulation and the resulting operation of bipolar dc grids has

to be further investigated. Finally, it is relevant to investigate distributed solutions in order to allow connected dc microgrids to robustly run their own economic dispatch and increase system resilience.

REFERENCES

- [1] L. Mackay, N. H. van der Blij, L. Ramirez-Elizondo, and P. Bauer, "Toward the Universal DC Distribution System," *Electric Power Components and Systems*, vol. 45, no. 10, pp. 1032–1042, 2017.
- [2] L. Mackay, T. G. Hailu, G. R. Chandra Mouli, L. Ramirez-Elizondo, J. A. Ferreira, and P. Bauer, "From DC Nano- and Microgrids Towards the Universal DC Distribution System A Plea to Think Further Into the Future," in *PES General Meeting*. IEEE, 2015.
- [3] R. Wiget and G. Andersson, "Optimal Power Flow for Combined AC and Multi-Terminal HVDC Grids based on VSC Converters," in *IEEE Power and Energy Society General Meeting*, 2015.
- [4] J. Beerten, S. Cole, and R. Belmans, "A sequential AC/DC power flow algorithm for networks containing Multi-terminal VSC HVDC systems," in *IEEE PES General Meeting*. IEEE, jul 2010, pp. 1–7.
- [5] J. Rimez and R. Belmans, "A combined AC/DC optimal power flow algorithm for meshed AC and DC networks linked by VSC converters," *International Transactions on Electrical Energy Systems*, vol. 25, no. 10, pp. 2024–2035, oct 2015.
- [6] L. Gan and S. H. Low, "Optimal Power Flow in Direct Current Networks," *IEEE Transactions on Power Systems*, vol. 29, no. 6, pp. 1–13, 2014.
- [7] Y.-K. Chen, Y.-C. Wu, C.-C. Song, and Y.-S. Chen, "Design and Implementation of Energy Management System With Fuzzy Control for DC Microgrid Systems," *IEEE Transactions on Power Electronics*, vol. 28, no. 4, pp. 1563–1570, apr 2013.
- [8] J. Ma, L. Yuan, Z. Zhao, and F. He, "Transmission Loss Optimization-Based Optimal Power Flow Strategy by Hierarchical Control for DC Microgrids," *IEEE Transactions on Power Electronics*, vol. 32, no. 3, pp. 1952–1963, mar 2017.
- [9] L. Mackay, A. Dimou, R. Guarnotta, G. Morales-Espania, L. Ramirez-Elizondo, and P. Bauer, "Optimal Power Flow in Bipolar DC Distribution Grids with Asymmetric Loading," in *IEEE Energycon Leuven*, 2016.
- [10] R. P. O'Neill, P. M. Sotkiewicz, B. F. Hobbs, M. H. Rothkopf, and W. R. S. Jr., "Efficient market-clearing prices in markets with nonconvexities," *European Journal of Operational Research*, vol. 164, no. 1, pp. 269 – 285, 2005.
- [11] G. Stamtzis, "Power transmission cost calculation in deregulated electricity market," Ph.D. dissertation, Universität Duisburg-Essen, 2003. [Online]. Available: <http://purl.oclc.org/NET/duett-12102003-112744>
- [12] T. Wu, M. Rothleder, Z. Alaywan, and A. D. Papalexopoulos, "Pricing Energy and Ancillary Services in Integrated Market Systems by an Optimal Power Flow," *IEEE Transactions on Power Systems*, vol. 19, no. 1, pp. 339–347, 2004.
- [13] Y. F. Y. Fu and Z. L. Z. Li, "Different models and properties on LMP calculations," *2006 IEEE Power Engineering Society General Meeting*, 2006.
- [14] D. Gautam and M. Nadarajah, "Influence of distributed generation on congestion and LMP in competitive electricity market," *World Academy of Science, Engineering and Technology*, vol. 39, no. 3, pp. 822–829, 2009.
- [15] M. S. H. Nabavi, S. Hajforoosh, and M. A. Masoum, "Placement and Sizing of Distributed Generation Units for Congestion Management and Improvement of Voltage Profile using Particle Swarm Optimization," *IEEE PES Innovative Smart Grid Technologies, ISGT Asia 2011 Conference: Smarter Grid for Sustainable and Affordable Energy Future*, 2011.
- [16] E. Litvinov, "Design and operation of the locational marginal prices-based electricity markets," *IET Generation, Transmission & Distribution*, vol. 4, no. 2, p. 315, 2010.
- [17] *GAMS: The Solvers Manuals*. GAMS, 2015, vol. CPLEX 12. [Online]. Available: <http://gams.com/help/topic/gams.doc/solvers/allsolvers.pdf>
- [18] L. Mackay, T. Hailu, L. Ramirez-Elizondo, and P. Bauer, "Decentralized Current Limiting in Meshed DC Distribution Grids," in *DC Microgrids, IEEE First International Conference on*, 2015.
- [19] P. Purgat, L. Mackay, R. Adilardi Prakoso, L. Ramirez-Elizondo, and P. Bauer, "Power flow control converter for meshed LVDC distribution grids," in *2017 IEEE Second International Conference on DC Microgrids (ICDCM)*. IEEE, jun 2017, pp. 476–483.